NANO LETTERS

pubs.acs.org/NanoLett

Letter

A Single-Molecule Strategy to Capture Non-native Intramolecular and Intermolecular Protein Disulfide Bridges

Marc Mora,* Stephanie Board, Olivier Languin-Cattoën, Laura Masino, Guillaume Stirnemann, and Sergi Garcia-Manyes*

Cite This: *Nano Lett.* 2022, 22, 3922−3930

Read Online

ACCESS | Metrics & More | Article Recommendations | Supporting Information

ABSTRACT: Non-native disulfide bonds are dynamic covalent bridges that form post-translationally between two cysteines within the same protein (intramolecular) or with a neighboring protein (intermolecular), frequently due to changes in the cellular redox potential. The reversible formation of non-native disulfides is intimately linked to alterations in protein function; while they can provide a mechanism to protect against cysteine overoxidation, they are also involved in the early stages of protein multimerization, a hallmark of several protein aggregation diseases. Yet their identification using current protein chemistry technology remains challenging, mainly because of their fleeting reactivity. Here, we use single-molecule spectroscopy AFM and molecular dynamics simulations to capture both intra- and intermolecular disulfide bonds in γD-crystallin, a cysteine-rich, structural human lens protein involved in age-related eye cataracts. Our approach showcases the power of mechanical force as a conformational probe in dynamically evolving proteins and presents a platform to detect non-native disulfide bridges with single-molecule resolution.

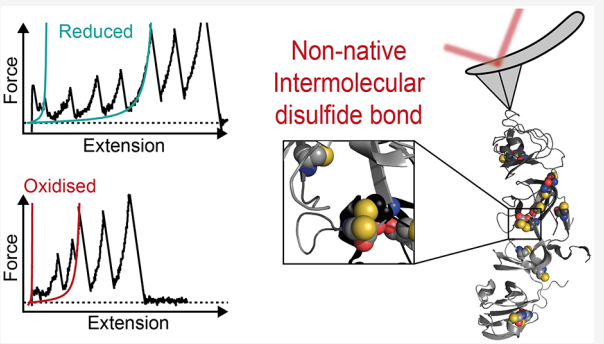

KEYWORDS: *protein nanomechanics, protein mechanochemistry, non-native disulfide bonds, single-molecule force spectroscopy, atomic force microscopy (AFM), protein folding*

INTRODUCTION

Native disulfide bridges—strong covalent bonds formed between two close cysteine residues—have been typically shown to provide structural stabilization to the folded conformation of proteins.[1,2] In addition to those disulfides with a clear structural—static—function, other intramolecular disulfide bonds display a dynamic behavior in virtue of their reversible thiol/disulfide chemistry, a mechanism that is collectively related to a myriad of redox-mediated signaling cellular processes,[3−5] and tightly modulated by the fluctuating redox properties of the environment and by dedicated oxidoreductase enzymes that ensure overall redox homeostasis.[6] A further layer of complexity is added when solvent-exposed cysteines establish intermolecular disulfide bonds with a neighboring protein.[7−9] While intermolecular disulfide bonds play decisive functional roles—for example, they work as protective mechanisms against cysteine irreversible overoxidation[10,11] but are also involved in a large number of aggregation misfolding reactions[12−14]—their extremely fleeting nature makes them challenging to detect experimentally. Several techniques, such as NMR have attempted to capture their presence in solution,[15] and a handful of crystal structures have provided the snapshots of a subset of (long-lived) stable conformations.[16] However, their markedly fast reactivity, underpinning their ability to multimerize in a (often) rather uncontrolled way, calls for the development of new experimental approaches enabling direct detection of non-native disulfide bonds.

Single-molecule force spectroscopy AFM has emerged as a powerful technique to identify intramolecular disulfide bonds,[17] which work as strong intramolecular staples. Typically, stretching a protein with an AFM extends it to almost its full contour length.[18] The presence of an intramolecular disulfide bond effectively shortcuts the protein, limiting its extensibility.[19] Hence, a shorter than expected increment of the protein's contour length can be considered as a reliable reporter of the presence of intramolecular disulfide bridges, as demonstrated in titin,[20,21] calmodulin binding domain,[22] FimG domain[23] and cell adhesion molecule domains.[24] Recent nanomechanical experiments also captured the dynamics of reduction and reformation of individual

Received: January 16, 2022
Revised: February 23, 2022
Published: May 12, 2022

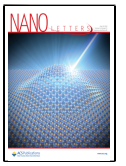

intramolecular disulfides by measuring the changes in protein extensibility over time.[25−30] Despite the unquestionable progress, this single-molecule approach is still not suitable to capture intermolecular, non-native disulfide bonds, notably because of the natural requirement of establishing a physical connection between (at least) two contacting proteins in the assay. Here, using a combination of protein engineering techniques (based on the rational design of polyproteins whereby the number of adjacent monomers prone to oxidation is precisely controlled), molecular dynamics (MD) simulations, and single-molecule force spectroscopy experiments, we develop an integrated single-molecule experimental approach able to capture both non-native inter- and intramolecular individual disulfide bonds, and characterize their dynamics under biologically mimicking redox conditions. We showcase our proof-of-principle experimental platform to study the complex redox reactivity of human γD-crystallin (γDc, a key human structural protein in the eye lens containing 6 reduced native cysteines), the aggregation of which[31−33]—intricately related to cysteine oxidation[32]—gives rise to the high-molecular weight protein aggregates that hallmark the eye's cataract disease.[34,35] Noteworthy, the ability to identify and trap non-native intermolecular disulfide bonds fingerprints a conformational change, involving the spontaneous and relatively frequent excursion of the native γD-crystallin to a well-defined intermediate conformation, that exposes to the solvent those natively cryptic (and thus unreactive) cysteines, becoming suddenly reactive. Besides enabling direct identification of non-native (intramolecular and intermolecular) disulfide bonds, our single-molecule strategy unambiguously captures disulfide-bond mediated protein dimerization and provides a direct probe of the subtle interplay between the redox status of a protein and its conformational dynamics.

RESULTS

Human γD-crystallin (γDc) is the third most abundant crystallin in the human lens,[36] which folds in the characteristic crystallin two-domain structure (Figure 1a). Despite its high degree of structural symmetry provided by its characteristic two Greek-key motifs, its cysteine content is not evenly distributed among the terminals. While the N-terminal domain (Ntd) harbors 4 cysteines, the C-terminal domain (Ctd) contains only two cysteines, arranged in a CXC motif, Figure 1b. In neither termini does the crystallized native structure show the presence of a disulfide bridge (PDB: 1HK0). Consequently, mechanical unfolding and stretching of a single γDc monomer with an AFM should uncomplicatedly elicit the whole length of the protein. To test this hypothesis, we first engineered a polyprotein construct whereby two γDc monomers are intercalated with the Ig91 marker protein, $(Ig91{-}\gamma Dc)_2$ (Figure 2a). This strategy enables the marker protein not only to serve as an internal mechanical fingerprint (the mechanical properties of the Ig91 protein have been well-characterized,[18] Supporting Figures 1 and 2) but also to avoid any physical interaction between the two γDc monomers. Stretching an individual $(Ig91{-}\gamma Dc)_2$ polyprotein at a constant velocity of 400 nm s^{-1} with an AFM commonly resulted in unfolding trajectories with (up to) four unfolding peaks prior to the two unfolding peaks of the Ig91 markers (Figure 2b, top). Each of the (Ntd and Ctd) termini within each γDc monomer unfolded independently, and the mechanical unfolding of the full $(Ig91{-}\gamma Dc)_2$ construct quantitatively agreed in terms of unfolding forces (F_{Ntd} = 131 ± 15 pN; F_{Ctd} = 100 ± 19 pN) and contour length increments ($\Delta L_{c,Ntd}$ = 29.0 ± 1.1 nm; $\Delta L_{c,Ctd}$ = 29.7 ± 1.0 nm) with the independent mechanical characterization of each individual terminus (Supporting Figure 3). Consequently, in the full $(Ig91{-}\gamma Dc)_2$ typical unfolding trajectory, the first two peaks (Figure 2b, top) corresponded to the unfolding of the mechanically weaker Ctds, followed by the unfolding of the two Ntds, displaying higher mechanical stability, before the unfolding of the higher mechanical stability Ig91 markers.

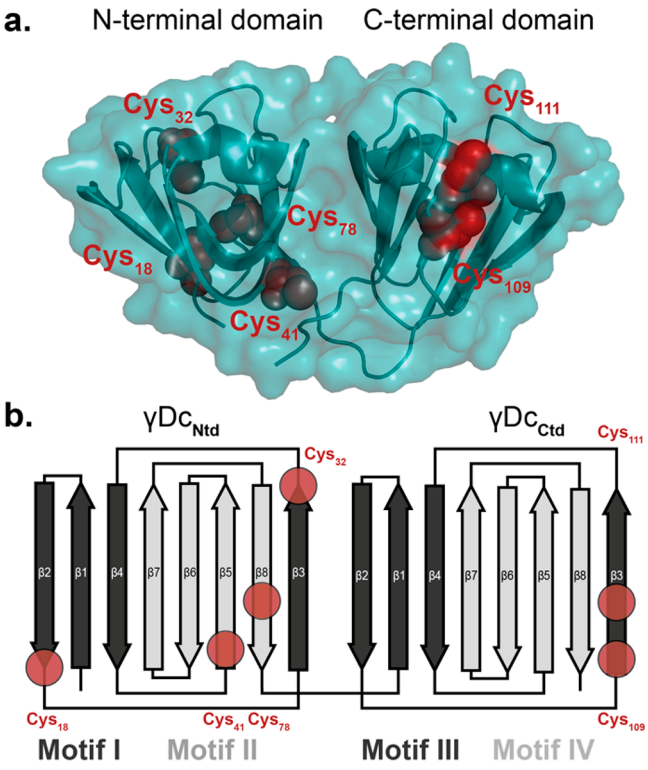

Figure 1. Cysteine content in γD-crystallin. (a) Cartoon representation of the γDc structure (PDB: 1HK0) harboring six reduced cysteines (red) unevenly distributed between the two protein termini. The two globular domains (N-terminal domain, Ntd; C-terminal domain, Ctd) fold independently and are joined by an unstructured 7-amino acid linker. (b) Schematic representation of the 4 characteristic Greek key motifs of the γDc (motifs I–IV), consisting of two intercalated antiparallel β-sheet motifs in each termini. Each red circle marks the location of the cysteines within the protein structure.

As expected, in the vast majority of the unfolding traces (91%) (Figure 2b, top) the total full γDc length ΔL_c ~120 nm is released upon unfolding, since each γDc terminal contributes with ~30 nm (4 termini × 30 nm = 120 nm, Supporting Figure 4). However, a few yet significant (9%) unfolding trajectories showed a marked reduction in the total $(\gamma Dc)_2$ ΔL_c unfolding length, $(\gamma Dc)_2$ ΔL_c < 120 nm (Figure 2b, bottom and Supporting Figures 5 and 6). To unambiguously resolve if such molecular shortening is the result of the formation of non-native disulfide bridges, we reproduced the experiments in a reduced environment (1 mM of deprotonated glutathione). Pulling the same $(Ig91{-}\gamma Dc)_2$ polyprotein (Figure 2a) in the presence of GSH confirmed the absence of trajectories featuring a reduction in the total $(\gamma Dc)_2$ extension (Figure 2c), strongly suggesting that the shorter unfolding trajectories obtained under oxidizing (PBS) conditions (Figure 2b, bottom) very likely correspond to the formation of (non-native) intramolecular disulfide bonds that are not found in the

https://doi.org/10.1021/acs.nanolett.2c00043
Nano Lett. 2022, 22, 3922−3930

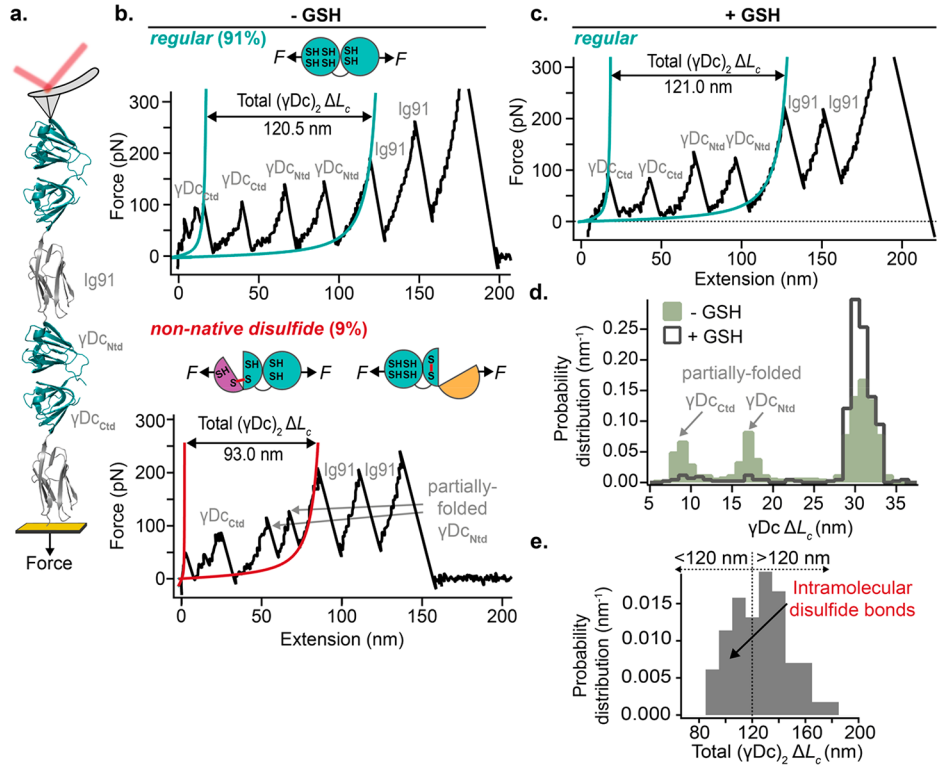

Figure 2. Capturing intramolecular non-native disulfide bonds. (a) Schematics of the single-molecule AFM experiment, whereby a single engineered (Ig91−γDc)$_2$ polyprotein is stretched between an AFM cantilever and a gold-coated cover slide. (b) Representative force−extension unfolding trajectories of the (Ig91−γDc)$_2$ polyprotein in the absence of reducing agent. The most common *regular* trajectory (top) displays the uncomplicated unfolding of the two mechanically weaker Ctds first, followed by the unfolding of the two Ntds, releasing a total ΔL_c of ∼120 nm (turquoise WLC fits). The last two unfolding events correspond to the unfolding of the Ig91 marker domains. The shorter force−extension trace (bottom) shows an overall reduction in the (γDc)$_2$ extension (<120 nm), reminiscent of intramolecular non-native disulfide bridge(s) formation. (c) In the presence of 1 mM of deprotonated GSH, only the *regular* phenotype is observed. (d) Histogram comparing the frequency of observed increment in contour-length in γDc corresponding to the stretching of (γDc−Ig91)$_2$ polyprotein in the presence and absence of GSH [n = 564 unfolding events without GSH (green) and n = 422 unfolding events with GSH (empty gray)]. (e) Histogram of the total increase in contour length, (γDc)$_2$ ΔL_c, when pulling (Ig91−γDc)$_2$ in the absence of a reducing agent (n = 114 unfolding trajectories).

native crystal structure (Figure 1). Close inspection to the contour length histogram associated with crystallin unfolding (Figure 2d) revealed a predominant peak at ∼30 nm, likely corresponding to the all-or-none unfolding of each individual domain, in addition to two extra lower occurrence peaks at shorter lengths (ΔL_c ∼15 and ∼9 nm) that correspond to the unfolding of well-defined partially folded conformations occurring in the Ntd (ΔL_c ∼15 nm and ∼130 pN) or the Ctd (ΔL_c ∼9 nm and ∼155 pN), clearly distinguishable when pulling both γDc terminals independently (Supporting Figure 3). Remarkably, the relative abundance of both peaks is dramatically reduced under reducing conditions, while the probability of observing a ∼30 nm full-length unfolding event is instead increased. Combined, these experiments suggest that those shorter trajectories (Figure 2b, bottom) leading to protein extensions shorter than ∼120 nm (Figure 2e) are directly related to the mechanical intermediate conformations that largely resolve upon GSH addition.

Having observed that γDc forms non-native intramolecular disulfide bonds, we questioned whether γDc can also establish intermolecular disulfide bonds with neighboring monomers. To this purpose, we built a polyprotein construct whereby two γDc monomers are physically connected to each other and flanked by the Ig91 marker proteins (Figure 3a). Pulling on the resulting Ig91−(γDc)$_2$−Ig91 polyprotein resulted in a rich repertoire of unfolding trajectories, that could be classified into three mechanical phenotypes. In most cases (55%, Figure 3b, top), a *regular* (and expected) full-length unfolding trajectory consisting of four independent unfolding events of ∼30 nm (Supporting Figure 7) was observed. We also identified two distinct unexpected unfolding pathways that markedly departed from this *regular* behavior. First, around 23% of the trajectories exhibited a well-defined unfolding pattern (Figure 3b, middle), where the typical mechanical hierarchy is lost, exhibiting unfolding peaks of alternating higher and lower mechanical stabilities. This unfolding scenario is overall compatible with γDc dimerization through a domain swap mechanism via Ntd interchange that we described earlier.[37] Importantly, the unfolding pattern does not exhibit any shortening in the (γDc)$_2$ length, implying that domain swap-mediated dimerization maintains the native redox status of all 12 cysteines comprised in the two γDc monomers (Supporting Figure 8). The remaining 22% of the unfolding trajectories featured a significant decrease in the total (γDc)$_2$ unfolding length (Figure 3b, bottom), which is likely to be underpinned by the formation of non-native disulfide bridges. Direct comparison of the measured total ΔL_c(γDc)$_2$ for the Ig91−(γDc)$_2$−Ig91 polyprotein and the previously characterized (Ig91−γDc)$_2$ construct enabled us to directly identify whether the formation of non-native disulfide bridges occurs within the same protein or between the two adjacent γDc monomers, Figure 3c. We conclude that, when the total ΔL_c (γDc)$_2$ is

https://doi.org/10.1021/acs.nanolett.2c00043
Nano Lett. 2022, 22, 3922−3930

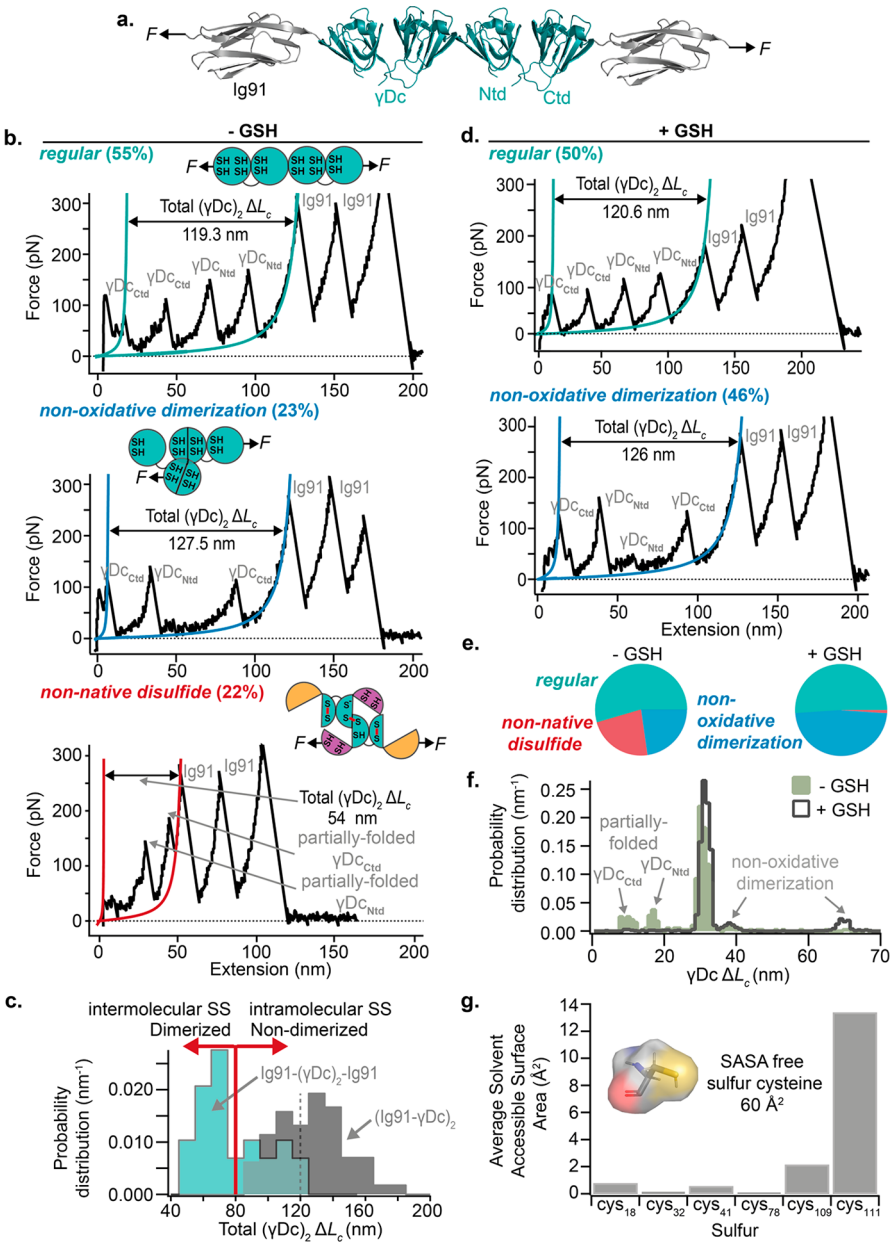

Figure 3. Capturing non-native intermolecular disulfide bridges in γDc. (a) Schematics of the engineered Ig91−$(\gamma Dc)_2$−Ig91 polyprotein, containing two physically interacting γDc monomers. (b) Pulling on an individual Ig91−$(\gamma Dc)_2$−Ig91 polyprotein at a constant velocity and in the absence of GSH results in three different unfolding phenotypes according to their length and peak position—*regular* (top), *non-oxidative dimerization* (middle), and *non-native disulfide* (bottom). The percentage values in brackets represent the frequency of each length phenotype. The *regular* unfolding trajectories (top) exhibit the initial unfolding of the two γDc monomers, releasing a total length of 120 nm. The *non-oxidative dimerization* length phenotype (middle) usually entails four γDc unfolding events with varying ΔL_c values and mechanical stabilities. The overall total ΔL_c $(\gamma Dc)_2$ extension is larger than the *regular* phenotype by 7 nm. (c) Histogram comparing the total γDc $(\Delta L_c)_2$ when pulling Ig91−$(\gamma Dc_{WT})_2$−Ig91 (turquoise) and $(Ig91-\gamma Dc_{WT})_2$ (gray) enabling to discriminate between (red vertical line) intramolecular (total γDc $(\Delta L_c)_2$ > 80 nm) and intermolecular (total γDc $(\Delta L_c)_2$ < 80 nm) non-native disulfide bridge formation in the absence of GSH. The *non-native disulfide* length phenotype (middle) typically displays a shorter total ΔL_c $(\gamma Dc)_2$ extension and usually features partially folded conformations originating from either terminal. (d) Pulling on the Ig91−$(\gamma Dc)_2$−Ig91 polyprotein in the presence of 1 mM of deprotonated GSH results in only two length γDc phenotypes: the *regular* (top) and the non-oxidative dimerization (bottom) unfolding pattern. (e) Pie charts showing the comparison between the different unfolding length phenotypes captured with and without GSH. (f) Histogram comparing the frequency of the γDc increment in contour-length when pulling the Ig91−$(\gamma Dc)_2$−Ig91 polyprotein with and without GSH (n = 400 unfolding events without GSH and n = 1387 unfolding events with GSH). (g) Average sulfur solvent accessible surface area (SASA) of the 6 different cysteines comprised in γDc_{WT}.

shorter than 80 nm (light blue part of the histogram in Figure 3c), the two neighboring γDc monomers have dimerized through the formation of, at least, one non-native intermolecular disulfide bridge.

Examining the nanomechanical response of the same Ig91−$(\gamma Dc)_2$−Ig91 polyprotein in the presence of reduced GSH (and TCEP, Supporting Figure 9) resulted in the absence of the shorter unfolding length phenotype, confirming that the formation of non-native disulfide bonds account for the

https://doi.org/10.1021/acs.nanolett.2c00043
Nano Lett. 2022, 22, 3922−3930

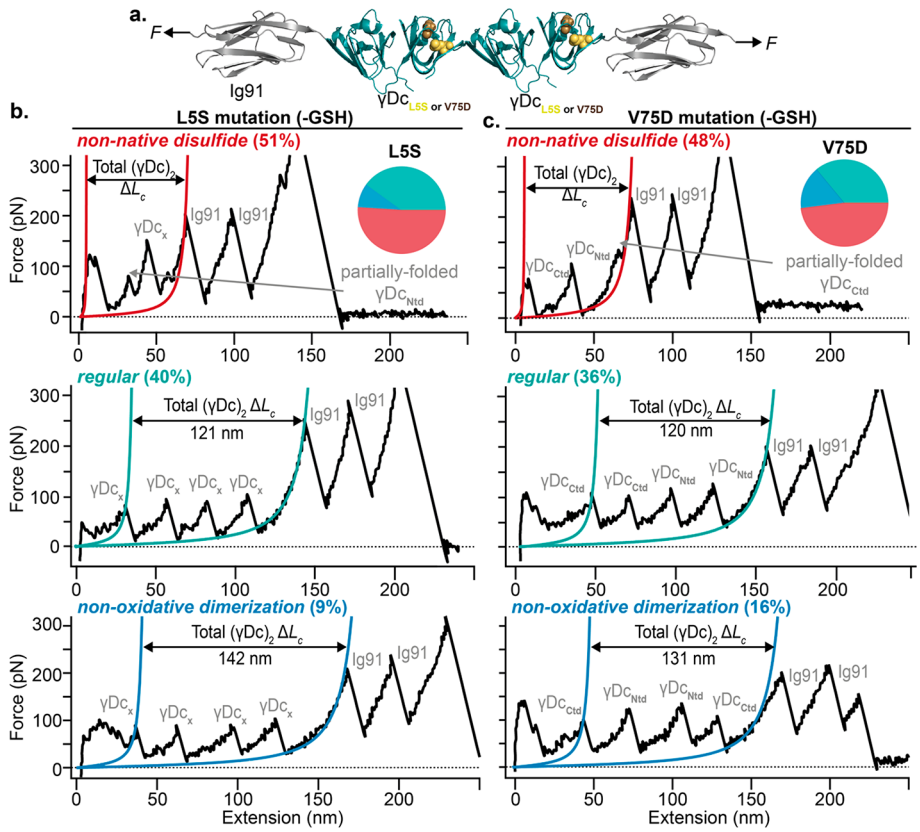

Figure 4. Single-point mutations enhance the formation of non-native intra- and intermolecular disulfide bridges. (a) Schematics of the engineered Ig91−$(\gamma Dc_{L5SorV75D})_2$−Ig91 polyproteins. (b) Pulling on the polyprotein construct harboring the L5S congenital mutation in each γDc monomer results in unfolding trajectories featuring three different length phenotypes—*non-native disulfide* (top), *regular* (middle), and *non-oxidative dimerization* (bottom). (c) Pulling on a related single polyprotein construct harboring the V75D congenital mutation displays force−extension unfolding trajectories populating the three different length phenotypes—*non-native disulfide* (top), *regular* (middle), and *non-oxidative dimerization* (bottom).

shortening in $(\gamma Dc)_2$ extension. Under these reducing conditions, the two other unfolding phenotypes, namely the *regular* (Figure 3d, top) and the non-oxidative dimerization pathway (Figure 3d, bottom) were observed in an almost equal probability (Figure 3e). As before, the histogram of γDc ΔL_c clearly shows that the population of partially folded conformations vanishes after exposure to reducing conditions, while the ΔL_c defining the domain swapped conformation increases its probability of occurrence (Figure 3f).

The first obvious and unavoidable requirement for the formation of intermolecular disulfide bonds is that the involved cysteines from both neighboring proteins are surface-exposed. To evaluate the degree of sulfur exposure of the 6 different cysteines in each γDc monomer we conducted MD simulations, which demonstrated that only the sulfur in cys^{111} (in the Ctd) is partially exposed to the environment, while the other 5 cysteines are completely buried in the folded structure (Figure 3g). This finding suggests that, for the intermolecular disulfide bonds to occur, the individual γDc monomers need to undergo a conformational change (in the absence of force) that destabilizes the protein, ultimately resulting in cysteine exposure to the solvent. With this rationale in mind, we aimed to elucidate whether protein destabilization enhances non-native intermolecular disulfide formation. Given that 4 of the cysteines in γDc are present in the N-terminal, where, incidentally, most of the congenital cataract-point mutations cluster,[38,39] we hypothesized that the introduction of single-point mutations in the Ntd could lead to destabilization, hence increasing the probability of cysteine exposure. We, first, used MD simulations to compare the sulfur solvent accessibility of the cysteines in the wild-type form with those in two pathogenic mutants, L5S and V75D,[40] which overall did not show any significant change in the sulfur accessibility (Supporting Figure 10). We then constructed two different polyprotein constructs (Ig91−$(\gamma Dc_{L5S})_2$−Ig91 and Ig91−$(\gamma Dc_{V75D})_2$−Ig91) independently harboring each congenital cataract point mutation (Figure 4a). Pulling on the Ig91−$(\gamma Dc_{L5S})_2$−Ig91 polyprotein in an oxidizing (PBS) environment (Figure 4b) revealed that the most prevalent pathway (50%) corresponded to the unfolding trajectories featuring a reduction in the overall $(\gamma Dc)_2$ length, reminiscent of the formation of non-native disulfide bridges. The second most captured unfolding pathway (42%) followed the *regular* mechanical unfolding, and only 8% of the unfolding trajectories displayed the non-oxidative domain-swap dimerization unfolding pattern (Supporting Figure 11b). Noteworthy, for this L5S mutant, the mechanical stability of the Ntd is significantly decreased with respect to the wild-type protein, probably due to fact that the L5S mutation is located on the first β-strand of the Ntd (the protein's mechanical clamp), making both protein terminals mechanically indistinguishable (Supporting Figure 12). Pulling on the Ig91−$(\gamma Dc_{V75D})_2$−Ig91 protein (Figure 4c) gave rise to very similar results, whereby the predominant unfolding pathway (48%)

https://doi.org/10.1021/acs.nanolett.2c00043
Nano Lett. 2022, 22, 3922−3930

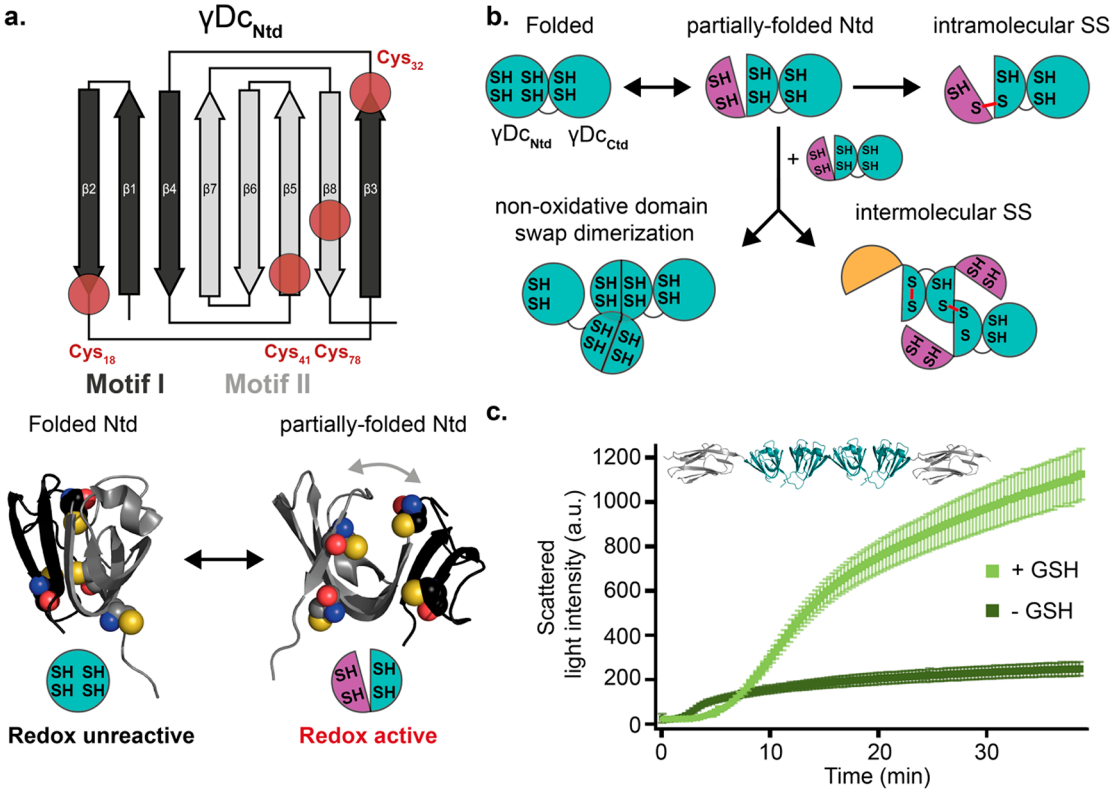

Figure 5. Spontaneous Ntd conformational switch reveals cryptic cysteines and enables their reactivity. (a) Plausible structural change spontaneously undergone by γDc Ntd, involving a partially folded conformation characterized by the hinge-like detachment of motif I from motif II, resulting in the concomitant solvent-exposure of at least three cysteines that become suddenly reactive. (b) Schematic mechanistic representation of the cysteine-redox regulated conformational diversity encountered in γDc. (c) Aggregation kinetics of the Ig91−$(\gamma Dc)_2$−Ig91 polyprotein in the presence and absence of GSH, measured by light scattering at 60 °C GSH (n = 4 for each condition, error bars s.e.m.).

comprises unfolding trajectories featuring a shorter $(\gamma Dc_{V75D})_2$ unfolding length, followed by the *regular* (36%) and domain swapped (16%) unfolding phenotypes (Supporting Figure 11c). Following a similar approach to that followed in Figure 3c, the measured ΔL_c $(\gamma Dc_X)_2$ histogram reveals that, for both protein mutants, the proportion of intra- and intermolecular non-native disulfide formation is roughly the same (Supporting Figure 13). Combined, these experiments point toward an enticing scenario, where the lower thermodynamic stability of the Ntd domain of the protein mutants[38] would enhance a conformational change that would expose previously buried cysteines, increasing the probability of non-native disulfide bond formation—a situation that becomes prevalent.

DISCUSSION

Whether beneficial or deleterious for the cell,[41,42] the detection of non-native, redox-regulated disulfide bridges has been particularly challenging. To date, most of the relevant studies use refined proteomics methods to tag[43] and capture these low-probability covalent bonds. Their highly dynamic nature, their fast reactivity, and their intimate relationship with the dynamically evolving protein structure necessitates the development of complementary experimental approaches.

Here, we use single-molecule force spectroscopy combined with protein engineering as a tool to capture non-native disulfide bonds by using molecular extensibility as their structural fingerprint. This methodology could be applied to virtually any protein, regardless of whether its physiological function is mechanical or not. As a proof-of-principle, we studied the redox-regulation of human γD-crystallin (γDc), the misfolding of which is directly related to eye's cataract. Our single-molecule experiments reveal the presence of both inter- and intramolecular non-native disulfide bonds in γDc. Pulling on the $(Ig91-\gamma Dc)_2$ polyprotein revealed the presence of non-native intramolecular disulfide bonds, directly linked to the existence of partially folded conformations found in both γDc_{Ctd} and γDc_{Ntd} domains. The γDc_{Ctd} has only two cysteines (cys^{109} and cys^{111}), a priori limiting the possible non-native disulfide bonds to the one (cys^{109}−cys^{111}) proposed by Serebryany et al.[44] However, the predominant intermediate conformation in γDc_{Ctd} is characterized by ΔL_c ∼9 nm, which would correspond to a "trapped length" much larger than that corresponding to the (cys^{109}−cys^{111}) disulfide (Supporting Figure 14). To rationalize this, we conducted MD simulations, showing that the formation of the non-native disulfide bridge in the γDc_{Ctd} can indeed induce a non-native partially folded protein conformation (Supporting Figure 15) compatible with the ΔL_c ∼9 nm that we observe. This change in γDc_{Ctd} conformation enforced by the formation of the non-native disulfide bridge is also likely accountable for the higher mechanical stability of the partially folded conformation (∼150 pN) when compared to the folded γDc_{Ctd} structure (∼100 pN). A closer look into the γDc_{Ntd} structure shows that the 4 cysteines are distributed evenly among the two Greek key motifs. Given that γDc_{Ntd} shows a partially folded conformation characterized by a ΔL_c ∼15 nm, a plausible scenario entails visiting a partially folded conformation whereby motif I is unfolded, while motif II remains folded (Supporting Figure 16). This partially folded conformation completely exposes

https://doi.org/10.1021/acs.nanolett.2c00043
Nano Lett. 2022, 22, 3922−3930

three cysteines (cys[18], cys[32], and cys[41]), which could explain the presence of both intramolecular and intermolecular disulfide bonds, the latter being uncovered when pulling on the Ig91−(γDc)$_2$−Ig91 polyprotein. Given that our molecular dynamics simulations revealed that, in the folded form, only one cysteine in the Ctd is solvent-accessible, it is highly plausible that a conformational change (which we speculate involves the spontaneous unfolding of half of the Ntd) that exposes cryptic cysteines is a necessary step prior to disulfide bond formation. Interestingly, the partial unfolding of the Ntd motif I was suggested to swap with a neighboring γDc domain.[37] We, therefore, propose a plausible global scenario able to explain the three observed types of non-native conformations; if γDc remains in the native state, it exhibits a *regular* pattern of unfolding. However, once the protein undergoes a conformational change involving a "hinge" that opens Ntd motif I (Figure 5a), then two competing situations emerge. Either the protein swaps with a neighboring domain (eliciting the domain swapped conformations), or it forms non-native disulfide bonds (either intra- or intermolecular), marked by the "shorter" unfolding phenotype (Figure 5b).

An intrinsic limitation of our approach is that, given the number of cysteines present in each γDc monomer, and hence of possible disulfide cross-links, we do not have the resolution to identify which cysteine pairs are involved in each particular non-native disulfide bond formed between adjacent domains. The intrinsic design of the polyprotein chain is also likely to restrict the number of possible intermolecular disulfide bonds, if compared to the much larger number of available conformations when the interacting monomers are in solution. Conversely, the polyprotein approach has the advantage of offering unprecedented control over the onset of protein misfolding, occurring at the dimer level. Functionally, it remains unknown what is the relationship between non-native disulfides and domain swapped structures. In the presence of GSH (Figure 3e) the population of "non-native disulfide trajectories" disappears, while the domain swapped population grows by essentially the same amount (from ∼20% to ∼50%), hence suggesting that these two conformations are in dynamic competition. As a first step toward relating these single-molecule observations to bulk aggregation measurements, we measured the kinetics of light scattering of the Ig91−(γDc)$_2$−Ig91 polyprotein in the absence and presence of reduced GSH (Figure 5c). Our results showed a drastic increase in the aggregation of the Ig91−(γDc)$_2$−Ig91 polyprotein in the presence of GSH, strongly suggesting that the non-native disulfide bonds that we measured at the single-molecule level act as a safety mechanism that prevents protein aggregation, probably by limiting the misfolded, domain swapped conformation that leads to protein aggregation. From the physiological perspective, given that the eye lens are separate from the blood vessels and lack protein regeneration machinery, and that its glutathione concentration unavoidably diminishes over time,[45] it is tempting to speculate that the amount of non-native disulfide bonds, which is one of the key initial steps toward developing cataracts,[46] will increase over the life-span of the individual.

Altogether, our experiments demonstrate the power of single-molecule spectroscopy to capture non-native disulfide bonds, both intra- and also intermolecular, by using the protein extension as a conformational reporter. In the specific case of γDc, non-native disulfide formation is likely to follow from a stochastic yet well-defined conformational excursion of the Ntd to a partially folded conformation that exposes previously cryptic cysteines to the solvent, hence rendering them reactive. We anticipate that our combined experimental platform, encompassing protein engineering, single-molecule force spectroscopy experiments, MD simulations and classical biochemistry techniques can help uncover the dynamic nature of non-native protein disulfide bonds, of wide occurrence in nature.

■ ASSOCIATED CONTENT

Supporting Information

The Supporting Information is available free of charge at https://pubs.acs.org/doi/10.1021/acs.nanolett.2c00043.

Details of polyprotein engineering, single-molecule AFM setup and data analysis, light-scattering experiments, molecular dynamics simulations, and additional data sets (PDF)

■ AUTHOR INFORMATION

Corresponding Authors

Marc Mora − *Department of Physics, Randall Centre for Cell and Molecular Biophysics and London Centre for Nanotechnology, King's College London, WC2R 2LS London, United Kingdom; Single Molecule Mechanobiology Laboratory, The Francis Crick Institute, London NW1 1AT, London, United Kingdom*; Email: marc.mora_hortal@kcl.ac.uk

Sergi Garcia-Manyes − *Department of Physics, Randall Centre for Cell and Molecular Biophysics and London Centre for Nanotechnology, King's College London, WC2R 2LS London, United Kingdom; Single Molecule Mechanobiology Laboratory, The Francis Crick Institute, London NW1 1AT, London, United Kingdom;* orcid.org/0000-0001-5140-2606; Email: sergi.garcia-manyes@kcl.ac.uk

Authors

Stephanie Board − *Department of Physics, Randall Centre for Cell and Molecular Biophysics and London Centre for Nanotechnology, King's College London, WC2R 2LS London, United Kingdom; Single Molecule Mechanobiology Laboratory, The Francis Crick Institute, London NW1 1AT, London, United Kingdom*

Olivier Languin-Cattoën − *CNRS Laboratoire de Biochimie Théorique, Institut de Biologie Physico-Chimique, Université Paris Diderot, Sorbonne Paris Cité, PSL Research University, 75005 Paris, France*

Laura Masino − *Structural Biology Science Technology Platform, The Francis Crick Institute, London NW1 1AT, United Kingdom*

Guillaume Stirnemann − *CNRS Laboratoire de Biochimie Théorique, Institut de Biologie Physico-Chimique, Université Paris Diderot, Sorbonne Paris Cité, PSL Research University, 75005 Paris, France;* orcid.org/0000-0002-5631-5699

Complete contact information is available at: https://pubs.acs.org/10.1021/acs.nanolett.2c00043

Author Contributions

S.G.M. and M.M. designed research. M.M. conducted single-molecule mechanical experiments and analyzed data. S.B. expressed and purified polyprotein constructs. G.S. and O.L.-C. performed and analyzed MD simulations. M.M. and L.M. performed and analyzed bulk aggregation experiments. M.M.

https://doi.org/10.1021/acs.nanolett.2c00043
Nano Lett. 2022, 22, 3922−3930

and S.G.M wrote the paper. All authors contributed to revising and editing the manuscript.

Notes

The authors declare no competing financial interest.

■ ACKNOWLEDGMENTS

We thank Ainhoa Lezamiz, Dr. Palma Rico, and Dr. Elena Rostkova for protein expression and purification. M.M. was funded by a Fight for Sight PhD studentship. This work was supported in part by the Francis Crick Institute, which receives its core funding from Cancer Research U.K. (FC001002), the U.K Medical Research Council (FC001002), and the Wellcome Trust (FC001002). For the purpose of Open Access, the author has applied a CC BY public copyright license to any Author Accepted Manuscript version arising from this submission. This work was supported by the European Commission (Mechanocontrol, Grant Agreement 731957), BBSRC sLOLA (BB/V003518/1) Leverhulme Trust Research Leadership Award RL-2016-015, Wellcome Trust Investigator Award 212218/Z/18/Z, and Royal Society Wolfson Fellowship RSWF/R3/183006 all to S.G.-M.

■ REFERENCES

(1) Graña-Montes, R.; Groot, N. S.; de Castillo, V.; Sancho, J.; Velazquez-Campoy, A.; Ventura, S. Contribution of Disulfide Bonds to Stability, Folding, and Amyloid Fibril Formation: The PI3-SH3 Domain Case. *Antioxid Redox Sign* **2011**, *16* (1), 1−15.

(2) Creighton, T. E. Disulphide Bonds and Protein Stability. *Bioessays* **1988**, *8* (2−3), 57−63.

(3) Schmidt, B.; Ho, L.; Hogg, P. J. Allosteric Disulfide Bonds †. *Biochemistry-us* **2006**, *45* (24), 7429−7433.

(4) Paulsen, C. E.; Carroll, K. S. Cysteine-Mediated Redox Signaling: Chemistry, Biology, and Tools for Discovery. *Chem. Rev.* **2013**, *113* (7), 4633−4679.

(5) Bechtel, T. J.; Weerapana, E. From Structure to Redox: The Diverse Functional Roles of Disulfides and Implications in Disease. *Proteomics* **2017**, *17* (6), 1600391.

(6) Wouters, M. A.; Fan, S. W.; Haworth, N. L. Disulfides as Redox Switches: From Molecular Mechanisms to Functional Significance. *Antioxid Redox Sign* **2010**, *12* (1), 53−91.

(7) Ohishi, K.; Nagamune, K.; Maeda, Y.; Kinoshita, T. Two Subunits of Glycosylphosphatidylinositol Transamidase, GPI8 and PIG-T, Form a Functionally Important Intermolecular Disulfide Bridge*. *J. Biol. Chem.* **2003**, *278* (16), 13959−13967.

(8) Majima, E.; Ikawa, K.; Takeda, M.; Hashimoto, M.; Shinohara, Y.; Terada, H. Translocation of Loops Regulates Transport Activity of Mitochondrial ADP/ATP Carrier Deduced from Formation of a Specific Intermolecular Disulfide Bridge Catalyzed by Copper-o-Phenanthroline (*). *J. Biol. Chem.* **1995**, *270* (49), 29548−29554.

(9) Li, P.; Wohland, T.; Ho, B.; Ding, J. L. Perturbation of Lipopolysaccharide (LPS) Micelles by Sushi 3 (S3) Antimicrobial Peptide the Importance of an Intermolecular Disulfide Bond in S3 Dimer for Binding, Disruption, and Neutralization of LPS*. *J. Biol. Chem.* **2004**, *279* (48), 50150−50156.

(10) Cremers, C. M.; Jakob, U. Oxidant Sensing by Reversible Disulfide Bond Formation*. *J. Biol. Chem.* **2013**, *288* (37), 26489−26496.

(11) Beedle, A. E. M.; Lynham, S.; Garcia-Manyes, S. Protein S-Sulfenylation Is a Fleeting Molecular Switch That Regulates Non-Enzymatic Oxidative Folding. *Nat. Commun.* **2016**, *7* (1), 12490.

(12) Li, Y.; Yan, J.; Zhang, X.; Huang, K. Disulfide Bonds in Amyloidogenesis Diseases Related Proteins. *Proteins Struct Funct Bioinform* **2013**, *81* (11), 1862−1873.

(13) Eisenberg, D.; Nelson, R.; Sawaya, M. R.; Balbirnie, M.; Sambashivan, S.; Ivanova, M. I.; Madsen, A. Ø.; Riekel, C. The Structural Biology of Protein Aggregation Diseases: Fundamental Questions and Some Answers. *Acc. Chem. Res.* **2006**, *39* (9), 568−575.

(14) Furukawa, Y.; Fu, R.; Deng, H.-X.; Siddique, T.; O'Halloran, T. V. Disulfide Cross-Linked Protein Represents a Significant Fraction of ALS-Associated Cu, Zn-Superoxide Dismutase Aggregates in Spinal Cords of Model Mice. *Proc. National Acad. Sci.* **2006**, *103* (18), 7148−7153.

(15) Kovermann, M.; Rogne, P.; Wolf-Watz, M. Protein Dynamics and Function from Solution State NMR Spectroscopy. *Q. Rev. Biophys.* **2016**, *49*, No. e6.

(16) Henzler-Wildman, K.; Kern, D. Dynamic Personalities of Proteins. *Nature* **2007**, *450* (7172), 964−972.

(17) Mora, M.; Stannard, A.; Garcia-Manyes, S. The Nanomechanics of Individual Proteins. *Chem. Soc. Rev.* **2020**, *49* (19), 6816.

(18) Rief, M.; Gautel, M.; Oesterhelt, F.; Fernandez, J. M.; Gaub, H. E. Reversible Unfolding of Individual Titin Immunoglobulin Domains by AFM. *Science* **1997**, *276* (5315), 1109−1112.

(19) Ainavarapu, S. R. K.; Brujić, J.; Huang, H. H.; Wiita, A. P.; Lu, H.; Li, L.; Walther, K. A.; Carrion-Vazquez, M.; Li, H.; Fernandez, J. M. Contour Length and Refolding Rate of a Small Protein Controlled by Engineered Disulfide Bonds. *Biophys. J.* **2007**, *92* (1), 225−233.

(20) Wiita, A. P.; Ainavarapu, S. R. K.; Huang, H. H.; Fernandez, J. M. Force-Dependent Chemical Kinetics of Disulfide Bond Reduction Observed with Single-Molecule Techniques. *Proc. National Acad. Sci.* **2006**, *103* (19), 7222−7227.

(21) Grützner, A.; Garcia-Manyes, S.; Kötter, S.; Badilla, C. L.; Fernandez, J. M.; Linke, W. A. Modulation of Titin-Based Stiffness by Disulfide Bonding in the Cardiac Titin N2-B Unique Sequence. *Biophys. J.* **2009**, *97* (3), 825−834.

(22) Junker, J. P.; Ziegler, F.; Rief, M. Ligand-Dependent Equilibrium Fluctuations of Single Calmodulin Molecules. *Science* **2009**, *323* (5914), 633−637.

(23) Alonso-Caballero, A.; Schönfelder, J.; Poly, S.; Corsetti, F.; Sancho, D. D.; Artacho, E.; Perez-Jimenez, R. Mechanical Architecture and Folding of *E. coli* Type 1 Pilus Domains. *Nat. Commun.* **2018**, *9* (1), 2758.

(24) Carl, P.; Kwok, C. H.; Manderson, G.; Speicher, D. W.; Discher, D. E. Forced Unfolding Modulated by Disulfide Bonds in the Ig Domains of a Cell Adhesion Molecule. *Proc. National Acad. Sci.* **2001**, *98* (4), 1565−1570.

(25) Beedle, A. E. M.; Mora, M.; Lynham, S.; Stirnemann, G.; Garcia-Manyes, S. Tailoring Protein Nanomechanics with Chemical Reactivity. *Nat. Commun.* **2017**, *8* (1), 15658.

(26) Beedle, A. E. M.; Mora, M.; Davis, C. T.; Snijders, A. P.; Stirnemann, G.; Garcia-Manyes, S. Forcing the Reversibility of a Mechanochemical Reaction. *Nat. Commun.* **2018**, *9* (1), 3155.

(27) Alegre-Cebollada, J.; Kosuri, P.; Rivas-Pardo, J. A.; Fernández, J. M. Direct Observation of Disulfide Isomerization in a Single Protein. *Nat. Chem.* **2011**, *3* (11), 882−887.

(28) Kosuri, P.; Alegre-Cebollada, J.; Feng, J.; Kaplan, A.; Inglés-Prieto, A.; Badilla, C. L.; Stockwell, B. R.; Sanchez-Ruiz, J. M.; Holmgren, A.; Fernández, J. M. Protein Folding Drives Disulfide Formation. *Cell* **2012**, *151* (4), 794−806.

(29) Wiita, A. P.; Perez-Jimenez, R.; Walther, K. A.; Gräter, F.; Berne, B. J.; Holmgren, A.; Sanchez-Ruiz, J. M.; Fernandez, J. M. Probing the Chemistry of Thioredoxin Catalysis with Force. *Nature* **2007**, *450* (7166), 124−127.

(30) Giganti, D.; Yan, K.; Badilla, C. L.; Fernandez, J. M.; Alegre-Cebollada, J. Disulfide Isomerization Reactions in Titin Immunoglobulin Domains Enable a Mode of Protein Elasticity. *Nat. Commun.* **2018**, *9* (1), 185.

(31) Kosinski-Collins, M. S.; King, J. In Vitro Unfolding, Refolding, and Polymerization of Human ΓD Crystallin, a Protein Involved in Cataract Formation. *Protein Sci.* **2003**, *12* (3), 480−490.

(32) Serebryany, E.; Woodard, J. C.; Adkar, B. V.; Shabab, M.; King, J. A.; Shakhnovich, E. I. An Internal Disulfide Locks a Misfolded Aggregation-Prone Intermediate in Cataract-Linked Mutants of Human ΓD-Crystallin*. *J. Biol. Chem.* **2016**, *291* (36), 19172−19183.

https://doi.org/10.1021/acs.nanolett.2c00043
Nano Lett. 2022, 22, 3922−3930

(33) Quintanar, L.; Domínguez-Calva, J. A.; Serebryany, E.; Rivillas-Acevedo, L.; Haase-Pettingell, C.; Amero, C.; King, J. A. Copper and Zinc Ions Specifically Promote Nonamyloid Aggregation of the Highly Stable Human γ-D Crystallin. *ACS Chem. Biol.* **2016**, *11* (1), 263−272.
(34) Héon, E.; Priston, M.; Schorderet, D. F.; Billingsley, G. D.; Girard, P. O.; Lubsen, N.; Munier, F. L. The γ-Crystallins and Human Cataracts: A Puzzle Made Clearer. *Am. J. Hum. Genet.* **1999**, *65* (5), 1261−1267.
(35) Roskamp, K. W.; Paulson, C. N.; Brubaker, W. D.; Martin, R. W. Function and Aggregation in Structural Eye Lens Crystallins. *Acc. Chem. Res.* **2020**, *53* (4), 863−874.
(36) Vendra, V. P. R.; Khan, I.; Chandani, S.; Muniyandi, A.; Balasubramanian, D. Gamma Crystallins of the Human Eye Lens. *Biochimica Et Biophysica Acta Bba - Gen Subj* **2016**, *1860* (1), 333−343.
(37) Garcia-Manyes, S.; Giganti, D.; Badilla, C. L.; Lezamiz, A.; Perales-Calvo, J.; Beedle, A. E. M.; Fernández, J. M. Single-Molecule Force Spectroscopy Predicts a Misfolded, Domain-Swapped Conformation in Human ΓD-Crystallin Protein*. *J. Biol. Chem.* **2016**, *291* (8), 4226−4235.
(38) Moreau, K. L.; King, J. Hydrophobic Core Mutations Associated with Cataract Development in Mice Destabilize Human ΓD-Crystallin. *J. Biol. Chem.* **2009**, *284* (48), 33285−33295.
(39) Ji, F.; Jung, J.; Koharudin, L. M. I.; Gronenborn, A. M. The Human W42R ΓD-Crystallin Mutant Structure Provides a Link between Congenital and Age-Related Cataracts. *J. Biol. Chem.* **2013**, *288* (1), 99−109.
(40) Whitley, M. J.; Xi, Z.; Bartko, J. C.; Jensen, M. R.; Blackledge, M.; Gronenborn, A. M. A Combined NMR and SAXS Analysis of the Partially Folded Cataract-Associated V75D ΓD-Crystallin. *Biophys. J.* **2017**, *112* (6), 1135−1146.
(41) Wedemeyer, W. J.; Welker, E.; Narayan, M.; Scheraga, H. A. Disulfide Bonds and Protein Folding †. *Biochemistry-us* **2000**, *39* (15), 4207−4216.
(42) Mossuto, M. F. Disulfide Bonding in Neurodegenerative Misfolding Diseases. *Int. J. Cell Biology* **2013**, *2013*, 318319.
(43) Borges, C. R.; Sherma, N. D. Techniques for the Analysis of Cysteine Sulfhydryls and Oxidative Protein Folding. *Antioxid Redox Sign* **2014**, *21* (3), 511−531.
(44) Serebryany, E.; Yu, S.; Trauger, S. A.; Budnik, B.; Shakhnovich, E. I. Dynamic Disulfide Exchange in a Crystallin Protein in the Human Eye Lens Promotes Cataract-Associated Aggregation. *J. Biol. Chem.* **2018**, *293* (46), 17997−18009.
(45) Fan, X.; Monnier, V. M.; Whitson, J. Lens Glutathione Homeostasis: Discrepancies and Gaps in Knowledge Standing in the Way of Novel Therapeutic Approaches. *Exp. Eye Res.* **2017**, *156*, 103−111.
(46) Truscott, R. J. W. Age-Related Nuclear Cataract—Oxidation Is the Key. *Exp. Eye Res.* **2005**, *80* (5), 709−725.

https://doi.org/10.1021/acs.nanolett.2c00043
Nano Lett. 2022, 22, 3922−3930